Multifractal behavior of the surfaces evolved with surface relaxation

Pradipta Kumar Mandal and Debnarayan Jana*
Department of Physics, University of Calcutta, 92 A.P.C. Road, Kolkata-700 009, India
(Received 19 February 2008; published 24 June 2008)

A discrete model exhibiting conserved dynamics with nonconserved noise involving particles of different nature, termed as linear and nonlinear, is proposed here. The morphology of the surface has been studied with different abundances of these particles. The saturated surface, slowly evolved from a lower contribution of nonlinear particles to a higher contribution of nonlinear particles, splits into four distinct scaling regimes with three crossover lengths. Each regime is characterized by different scaling property. It is shown that when the contribution of the nonlinear particles crosses a critical value, the surface morphology shows a linear-nonlinear "phase transition." The roughness exponent in a nonlinear regime is well compared with that of the continuum nonlinear equation in a molecular beam epitaxy (MBE) class as well as a MBE motivated discrete model.

DOI: 10.1103/PhysRevE.77.061604 PACS number(s): 81.15.Aa, 68.35.Ct, 61.43.Hv, 05.40.−a

I. INTRODUCTION

The study of the growth of rough surfaces and interfaces plays a major role in different phenomena of scientific interest and practical importance. In the last two decades, considerable progress has been achieved in the qualitative and quantitative study of kinetic roughening of rough surfaces and interfaces [1,2]. Such nonequilibrium rough surfaces and interfaces do appear in various physical, chemical, and biological systems. Examples include the growth of thin film by molecular beam epitaxy (MBE) [3,4], snowfall on a slanted glass window [5], piling of sand on a smooth surface [6], propagation of a fire front through a sheet of paper [7], fluid flow through porous media [8–10], and bacterial colony growth [11].

The scaling behavior of the growing interfaces can be studied through discrete models or by continuum equations [4]. Discrete models are defined by a set of deposition rules for the temporal and spatial evolution of the growing surfaces. The morphology of the growing surface is studied through its scaling property, defined by the Family-Vicsek phenomenological scaling law [12].

Another way to study the scaling behavior of a rough surface is through the stochastic growth equations [13], based on the generalized Langevin equation of the form

$$\frac{\partial h(\vec{x},t)}{\partial t} = G[h(\vec{x},t)] + \eta(\vec{x},t), \tag{1}$$

where $h(\vec{x},t)$ is the single-valued surface height function of the spatial coordinates $\vec{x}$ and time t, G is the deterministic growth term, and η is the noise. For linear growth, replacing the kernel term $G[h(\vec{x},t)]$ of equation (1) by $\nu\nabla^2 h$, one obtains the Edward-Wilkinson (EW) equation [14,15] and for $G[h(\vec{x},t)]=\nu\nabla^2 h+\frac{\lambda}{2}(\nabla h)^2$, the equation reduces to the Kardar-Parisi-Zhang nonlinear stochastic growth equation [16] as well.

The growth models involving the smallest possible particle size with the same or different kinds of growth mechanism have drawn much attention in literature [1,17–19]. Two different kinds of growth mechanisms are involved in several competitive growth models, such as (i) random deposition (RD) and random depositions with surface relaxation (RDSR) [20], (ii) ballistic deposition (BD) and RD [21], and (iii) Eden model (ED) and unstable Eden model (UED) [22]. Different kinds of particles are deposited with different probabilities. These competitive growth models show a scaling behavior depending upon the kind of particles which dominate over the others. All these models involve only two kinds of particles. Another model following a BD scheme involving two kinds of particles considered as "sticky" and "sliding" has also been reported [23,24].

Two nonequilibrium discrete solid on solid (SOS) models motivated by MBE surface growth were proposed by Wolf and Villian [25] and Das Sarma and Tamborenea (DT) [26]. These two models contain the essential property of surface relaxation in such a way that the particles diffuse to keep the number of their nearest neighbors maximum.

Motivated by all these discrete models, here we introduce a simple but interesting discrete model in terms of particle size, with different abundances. The basic diffusion mechanism of the RDSR model is kept intact. With the change of the size of the particles, the nonlinearity in the system is controlled. Here, the particles are restricted in three sizes deposited with three different probabilities. The scaling behavior of the generated complex surface can be expressed by a set of nontrivial characteristic exponents. The surface is shown to possess more than one fractal dimension. In particular, we point out clearly the role played by the particles, with different sizes in shaping the multifractal behavior of the surface.

The plan of the paper is as follows. In the next section we will describe the model and the relevant scaling properties to characterize the surface. In Sec. III, the numerical results corresponding to the scaling behavior of the surface are presented. We give a summary of our results and conclusions in Sec. IV.

II. DESCRIPTION OF THE MODEL AND DYNAMIC SCALING

The RDSR model with unique smallest possible particle size can be described as the diffusion of a particle along the

*djphy@caluniv.ac.in

surface up to a finite distance, after being deposited on a randomly chosen site on the surface. In other words, raining from the top in a straight line trajectory, the particles finally stick to the substrate according to the lower height distribution of the nearest neighbor columns [27] with a unity height increment ($|\Delta h|=1$). This mechanism can be effectively generalized by choosing the particle size not to be unique. Keeping this mechanism the same, we have modified the size of the particles in $(1+1)$ dimension.

We have taken a lattice of size L on which particles are deposited. The lattice can be thought of as a $1\times L$ matrix initially. Now the smallest possible particle that can be deposited will be a 1×1 matrix. Besides this, we have introduced two other types of particles with sizes 1×2 and 2×1. The rough surface is formed due to the RDSR aggregation mechanism followed by the particles of sizes 1×2, 2×1, and 1×1 with the deposition probabilities as p, q, and $[1-(p+q)]$, respectively.

The 2×1 particle may be thought as an attachment of two 1×1 particles up and down. If the 1×1 particle is represented as $\square$, then the 2×1 particle should look like

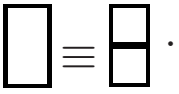

. This RDSR growth profile using the particle 2×1 is same as that of the particle 1×1 [27], except the height increment of the site on which the particle finally sticks is two units ($|\Delta h|=2$) instead of one.

Before discussion about the deposition of 1×2 particles we would like to define a term "stable position" corresponding to each such particle. If the 1×2 particle is thought of as an integration of two 1×1 particles side by side like

then stable position refers to a condition when at least two points from each of the two 1×1 particles touch other columns of the substrate lattice separately. In this circumstance, the selection of one 1×1 particle among the two 1×1 particles which build the 1×2 particle by the substrate lattice is random. This means the occurrence of each 1×1 particle is equally likely. The aggregation process of 1×2 particles can be described as follows—one of the two 1×1 particles of the 1×2 particle chooses a random site of the substrate lattice and then it (1×2 particle) searches for the lower height nearest neighbor columns with a stable position. The process is repeated until the 1×2 particle finds the stable position. For more clarification, one possible critical situation with two different equally probable cases [case (I) and case (II)] is demonstrated in Fig. 1. Here, the site **A** on the substrate is chosen randomly by a 1×2 particle constructed by two 1×1 particles, designated as **1** and **2** for distinction. This criteria forces the surface diffusion current to be inclination dependent. The lateral growth property due to the presence of 1×2 particles in the present model also breaks the up-down symmetry. So, nonlinearity due to the local slope (∇h) fluctuation should be included in the continuum description of this discrete model. It can thus be inferred that the surface

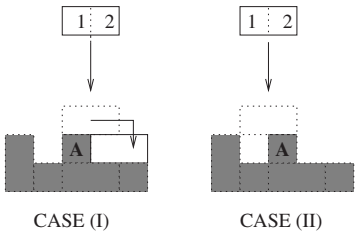

FIG. 1. Case (I) denotes the situation when 1, a 1×1 block of a 1×2 particle, is chosen by a random site **A** and case (II) is the situation when the other 1×1 block (marked as 2) of the 1×2 particle is chosen by the random site **A**.

formed by the significant contribution of the 1×2 particles will show more nonlinear scaling properties. Besides this, the shape of the 1×2 particles implies that the aggregation of such particles create "closed voids," avoiding possible overhangs. In this sense, 1×2 particles are termed as "nonlinear" ones.

The relaxation criteria has been introduced in this model in the following way. In view of the smallest particle (1×1), each particle is allowed to diffuse along the maximum number of nearest neighbors avoiding any irreversible sticking possibility. The diffusion of the 1×2 particle ensures that at least one of the two constituent 1×1 particles should get at least two nearest neighbors. The basic RDSR diffusion rules confirm that for a sufficient large time, the small slope approximation $|\nabla h|\ll 1$ is valid throughout the surface.

A typical deposition process with simultaneous involvement of the 1×2, 2×1, and 1×1 particles is shown in Fig. 2. The rough surface formed due to the simultaneous deposition of these three different types of particles with probabilities 0.5, 0.2, and 0.3 is shown in Fig. 3.

The development of the resulting rough surface can be well interpreted with the dynamic scaling concept, expressed as the space-time evolution of the surface width $w(t,L)$ following the Family-Vicsek scaling ansatz [12] as follows:

$$w(t,L)=[\langle h^2(x,t)\rangle-\langle h(x,t)\rangle^2]^{1/2}\sim L^{\alpha}f\left(\frac{t}{L^z}\right), \qquad (2)$$

where α is the roughness exponent, $z=\alpha/\beta$ (β is the growth exponent) and $f(u)$, the scaling function, behaves as $f(u)\sim u^{\beta}[u\ll 1]$, $f(u)\sim$ const $[u\gg 1]$ [1].

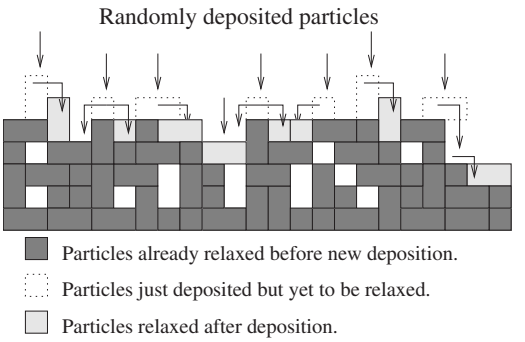

FIG. 2. The simultaneous deposition scheme of 1×1, 1×2, and 2×1 types of particles according to the RDSR rule.

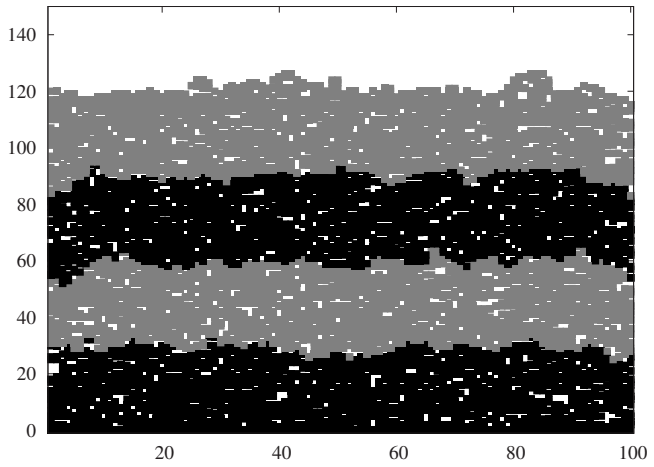

FIG. 3. The rough interface formed by the simultaneous deposition of the particles 1×2, 2×1, and 1×1, with the probabilities 0.5, 0.2, and 0.3, respectively. Here, the surface is obtained by the successive deposition of four sets of 25 000 particles, which are shown by different color shading.

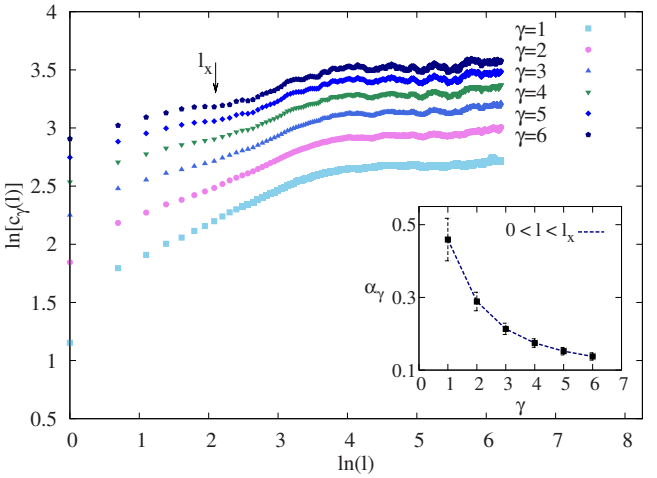

FIG. 4. (Color online) The γth-order correlation functions $c_\gamma(l)$ of the system having $p=0.2$, $q=0.2$ after $t=100$ monolayers of deposition. Inset: A variation of α_γ with γ is shown by the error bars.

The small and long wavelength fluctuations of the surface evolved in our present model can be better understood from the "multifractal" scaling of the rough surface. The concept of multifractality for self-affine surfaces provides us with deep insight into the complex nature of distributions and geometry [28]. In this context, it has been suggested [29] that for a class of surfaces, the γth-order height-height correlation functions should be studied which, for fixed time t in (1 +1) dimensions, are expected to exhibit the following scaling relation:

$$c_\gamma(l,t) = [\langle |h(x,t) - h(x+l,t)|^\gamma \rangle_l]^{1/\gamma} \sim l^{\alpha_\gamma}, \tag{3}$$

where α_γ is an exponent changing with γ. $\langle\ \rangle_l$ means the average over different windows of length l along the surface.

In our work we have taken a $(1+1)$-dimensional system having fixed size $L=1000$ with periodic boundary conditions and observed up to a time $t=10^5$ monolayers of depositions. Results are averaged over 10 independent runs.

III. RESULTS AND DISCUSSION

The temporal evolution of kinetic roughening of the surface with $p=0.2$ and $q=0.2$ (at different length scales) is demonstrated first. Initially after $t=100$ monolayers of deposition, the log-log plot of $c_\gamma(l)$ with length l for various values of γ is shown in Fig. 4.

It is seen from Fig. 4 that the height-height correlation is continued up to a length scale $l_s \sim t^{\beta/\alpha}$ with slow γ-dependent slope α_γ, corresponding to each $c_\gamma(l)$ (shown in the inset). The uncertainty of α_γ values due to the fitting of the function l^{α_γ} with $c_\gamma(l,t)$, are represented by error bars in the inset plot of α_γ vs γ. Beyond l_s, $c_\gamma(l)$ gets saturated, resulting in horizontal parallel lines. This observation clearly signifies that a weak mutifractal scaling regime exists up to l_s. No other length scale emerges except l_s until now.

Figure 5 presents the system in deep saturation after $t \sim 10^4$ monolayers of deposition. An important event is seen to occur; at this juncture a crossover length $l_\times$ emerges, below which a weak multifractal regime exists with different α_γ exponents (shown in the inset in Fig. 5).

A characteristic length scale $l_s \sim t^{\beta/\alpha}$ for a kinetic roughening process remains in marking the saturation of a system of size L; however, a new length scale $l_\times$ is required for distinguishing the multifractal and unifractal regimes. For $l > l_s$, no correlations exist due to the finite size of the system, resulting in saturation of the system. Therefore, the scaling behavior of the complex surface can be written mathematically as

$$c_\gamma(l) \sim l^{\alpha_\gamma} \quad \forall \quad \gamma \quad (\text{for } l < l_\times), \tag{4}$$

$$c_\gamma(l) \sim l^{\alpha} \quad \forall \quad \gamma \quad (\text{for } l_\times < l < l_s). \tag{5}$$

A rare event dominated growth process having a power law distribution of noise amplitudes [with μ as the decay expo-

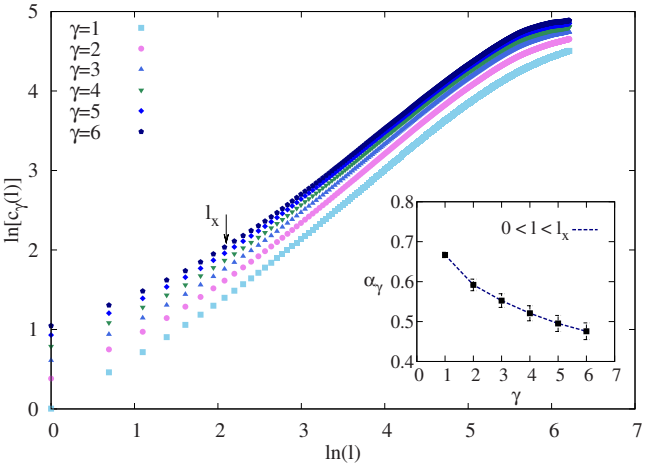

FIG. 5. (Color online) The γth-order correlation functions $c_\gamma(l)$ of the system having $p=0.2$, $q=0.2$ after $t\sim10^4$ monolayers of deposition. Inset: The slope of $c_\gamma(l)$ for different γ is plotted.

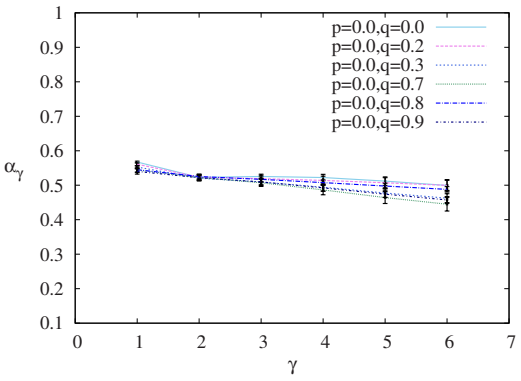

FIG. 6. (Color online) The exponent α_γ vs γ below $l_\times$ for the systems ($p=0.0$, $q=0.0$) and ($p=0.0$, $q=0.9$) after $t\sim 10^4$ monolayers of deposition.

nent like $P(\eta)\sim\eta^{-(1+\mu)}$ for $\eta>1$; $P(\eta)=0$ otherwise] shows strong multifractal behavior below a characteristic length scale depending upon the system size. It was shown that α_γ varies as $0.2<\alpha_\gamma<0.75$ when γ varies from 1 to 6 [28]. In comparison, the variation of α_γ in the present model is between $0.5<\alpha_\gamma<0.7$ when γ lies between $1<\gamma<6$, and implies a weak multifractal in nature. In spite of this similarity, the situation is different from that of a rare event controlled growth process [28]. The major difference is that the crossover length $l_\times$ in the present model is independent of system size L (not shown) and also p (see Fig. 9). The present multifractal behavior below the characteristic length scale $l_\times$ is best explained by the "intrinsic width" concept [30]. In general, the intrinsic width characterizes the internal structure of the surface and is seen to be independent of system size. Most probably, the intrinsic width originates from the voids, overhangs, and high steps present in the system. Krug [31] shows in a variant of the DT scheme that the nearest neighbor height-height correlation function has a time dependent nature as $c_\gamma(1,t)\sim[\langle|h(x,t)-h(x+1,t)|^\gamma\rangle_1]^{1/\gamma}\sim t^{\zeta_\gamma}$. This time dependent nature of $c_\gamma(1,t)$ is responsible for time dependent intrinsic width, which gives rise to this multifractal behavior.

The most relevant question to the present model is that of how the morphology of the surface is changing with p and q, a measure of nonlinearity in the system at the saturation limit.

To observe the effect of only 2×1 particles on the scaling properties of the rough surface below $l_\times$, we fix $p=0.0$, i.e., 1×2 particles are not involved in this process. Figure 6 shows the effect of q as the system proceeds from $q=0.0$ to $q=0.9$. It shows that in spite of the large change in q, the scaling property of the rough surface remains almost identical to that of the EW class with roughness exponent $\alpha_2\approx0.5$ [27]. No $l_\times$ appears here; the overall surface is uniaffine with $\alpha_\gamma\approx0.5$. It implies that, though the surface morphology evolves from ($p=0.0$, $q=0.0$) to ($p=0.0$, $q=0.9$), yet it remains in the EW class. It may be noted that the EW universality class is the characteristic of the surface generated only for $p=0.0$, $q=0.0$. The reason behind the uniformity of the evolution of the surfaces as ($p=0.0$, $q=0.0$)$\rightarrow$($p=0.0$, $q=0.9$) is that the basic relaxation belongs to the RDSR type with no inclination dependent surface diffusion current.

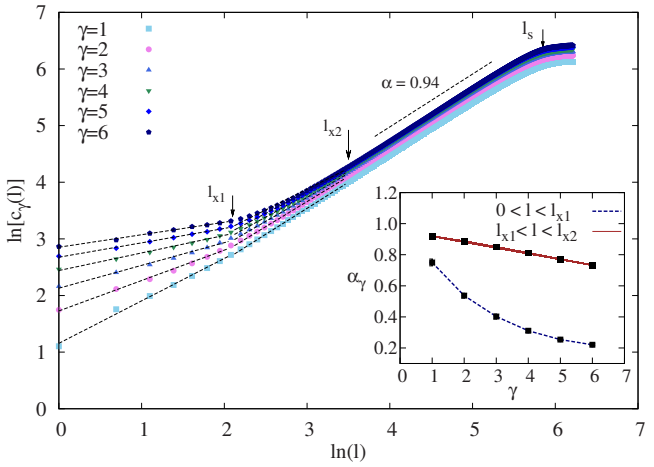

FIG. 7. (Color online) Log-log plot of correlation lengths $c_\gamma(l)$ for different γ with the power law fitting for the system with $p=1.0$ and $q=0.0$. Inset: The variation of the slope of $c_\gamma(l)$ with γ, one below $l_{\times1}$ and the other for $l_{\times1}<l<l_{\times2}$.

More interesting features emerge when the saturated surface (at around $t\sim10^4$) travels through different values of p, i.e., 1×2 particles are playing an increasingly significant and dominant role in shaping the morphology of the surface. Another system dependent characteristic length scale appears when p crosses a limiting value p_c. In this situation, the system seems to possess three different length scales $l_{\times1}$, $l_{\times2}$, and l_s. A complete description of these three length scales for the system $L=1000$, $p=1.0$, $q=0.0$ with the power law fitting are shown in Fig. 7. Two clear multifractal regimes, one is strong and the other weak, are noticed in the above figure. The slope variations of c_γ with γ in two different regimes separated by $l_{\times1}$ and $l_{\times2}$ is shown in the inset. Beyond $l_{\times2}$ the surface is "uniaffine" with the roughness exponent $\alpha=0.94\pm0.01$. This value is in good agreement with two discrete models; (i) a simple variant of the DT model [32] having roughness exponent $\alpha=1.05\pm0.10$ and (ii) conserved restricted solid on solid model [33] in (1+1) dimensions, having $\alpha=0.94\pm0.02$. Moreover, the dynamic renormalization group predicts $\alpha=1.0$ from the lowest-order nonlinear continuum MBE model exhibiting conserved dynamics with nonconserved noise as prescribed by Lai–Das Sarma [32] as follows:

$$\frac{\partial h}{\partial t}=-K\nabla^4h+\lambda_1\nabla^2(\nabla h)^2+\eta(\vec{x},t). \tag{6}$$

The similarity of the scaling behavior between the present model and that of Lai–Das Sarma [32] is because of the underlying fact that both the models have surface relaxation toward smaller height and large numbered nearest neighbor sites.

Above l_s no correlation exists. The birth of new crossover length $l_{\times2}$ is significant because it bridges the gap between the multiaffine nature of the surface to the uniaffine nature. It is interesting to see how the surface evolves from weak multiaffine to strong multiaffine below the crossover length $l_{\times1}$. In Fig. 8, α_γ is plotted against γ below $l_{\times1}$ as the surface is grown up with different deposition probabilities of 1×2 par-

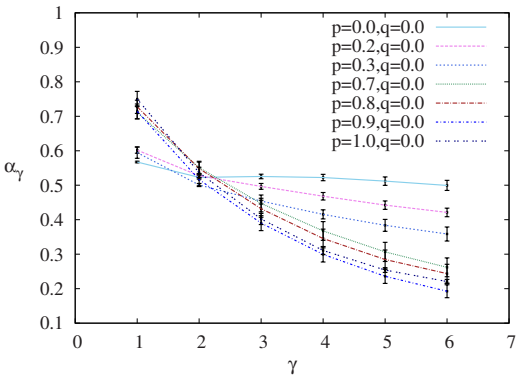

FIG. 8. (Color online) α_γ vs γ when the system proceeds from (p=0.0, q=0.0) to (p=1.0, q=0.0) after $t \sim 10^4$ monolayers of deposition.

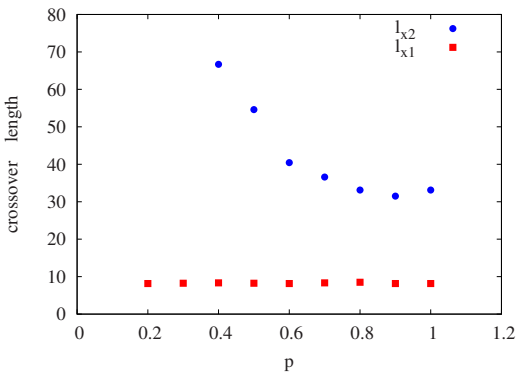

FIG. 9. (Color online) Plot of the two crossover lengths $l_{\times 1}$ and $l_{\times 2}$ with the 1×2 deposition probability p.

ticles. A clear signature of abrupt change in the α_γ values is noticed as the system crosses the limit p=0.3, and the surface becomes strong multiaffine. Besides the turbulent nature [31] of the surface beyond p=0.3, it is clearly seen that $\alpha_2 \approx 0.5$ for all p. It indicates that the linear RDSR scaling feature still exists below this length scale $l_{\times 1}$.

The formation of a new crossover characteristic length scale $l_{\times 2}$ shows a change in the scaling nature of the surface. It plays a crucial role in linking the multiaffine linear surface with the uniaffine nonlinear surface as discussed earlier. Naturally, the evolution of $l_{\times 2}$ will give a critical insight into the scaling behavior of the surface. In Fig. 9, $l_{\times 1}$ and $l_{\times 2}$ are plotted against p. It is clear from the figure that beyond p =0.3, the new crossover length $l_{\times 2}$ emerges creating a nonlinear regime. As the nonlinear particles (the 1×2 particle, designated as nonlinear because of the fact that this particle is solely responsible for introducing nonlinearity into the system) are introduced into the system, they face competition with the linear particles (the 1×1) to control the surface morphology. For $0.3 < p < 0.4$ there is a win of nonlinear particles over the linear ones beyond $l_{\times 2}$. Also, nonlinear particles play a definite role below $l_{\times 1}$, making the surface more turbulent in nature without nonlinearity. The situation around $0.3 < p < 0.4$ may be thought of as a linear-nonlinear phase transition beyond a system independent characteristic length scale $l_{\times 1}$, such that p as the order parameter and $l_{\times 2}$ as the observable. To observe the phase transition the critical value of p should remain within $0.3 < p_c < 0.4$.

IV. CONCLUSIONS

A discrete model exhibiting conserved dynamics with nonconserved noise involving particles of different sizes is introduced here. Two types of particles, linear and nonlinear, with different probability of deposition are taking part in the growth process. As the surface evolves gradually with time involving a major contribution from nonlinear particles, three distinct crossover lengths separate the overall surface into four scaling regimes. The lower regime shows a turbulent multifractal behavior. Next to that, a mixed nonlinear weak mutifractal regime occurs, which bridges the turbulent regime to a nonlinear unifractal regime. Beyond the unifractal regime, the usual saturation of the surface takes place. With the slow rate of increase in the involvement of nonlinear particles, the scaling properties of the saturated rough surface shows a linear-nonlinear phase transition beyond the mixed regime. Qualitatively, the phase transition is observed when the nonlinear particle has the deposition probability more than 0.3 but less than 0.4. The uniaffine surface, which is nonlinear in nature, satisfies the roughness exponent close to that predicted from the nonlinear MBE continuum equation.

ACKNOWLEDGMENTS

The authors gratefully acknowledge University Grant Commission (UGC), Government of India and DST-FIST for their financial support to carry out this work. It is a pleasure to thank A. K. Chaudhury School of Information Technology, University of Calcutta, India for their help in carrying out part of our simulation. We are thankful to an anonymous referee for pointing out several useful suggestions to improve the quality of the paper.

[1] A.-L. Barabási and H. E. Stanley, *Fractal Concepts in Surface Growth* (Cambridge University Press, Cambridge, New York, 1995).
[2] P. Meakin, Phys. Rep. **235**, 189 (1993).
[3] E. V. Albano, R. C. Salvarezza, L. Vázquez, and A. J. Arvia, Phys. Rev. B **59**, 7354 (1999).
[4] M. Kardar, Physica A **281**, 295 (2000).
[5] Z. Csahók and T. Vicsek, Phys. Rev. A **46**, 4577 (1992).
[6] P. Bak, C. Tang, and K. Wiesenfeld, Phys. Rev. Lett. **59**, 381 (1987).
[7] J. Zhang, Y.-C. Zhang, P. Alstrøm, and M. T. Levinsen, Physica A **189**, 383 (1992).

[8] M. Alava, M. Dubé, and M. Rost, Adv. Phys. **53**, 83 (2004).
[9] L. A. N. Amaral, A. L. Barabási, S. V. Buldyrev, S. Havlin, and H. E. Stanley, Phys. Rev. Lett. **72**, 641 (1994).
[10] P. B. S. Kumar and D. Jana, Physica A **224**, 199 (1996).
[11] E. Ben-jacob, O. Schochet, A. Tenenbaum, I. Cohen, A. Czirók, and T. Vicsek, Fractals **2**, 15 (1994).
[12] F. Family and T. Vicsek, J. Phys. A **18**, L75 (1985).
[13] M. Marsili, A. Maritan, F. Toigo, and J. R. Banavar, Rev. Mod. Phys. **68**, 963 (1996).
[14] S. T. Chui and J. D. Weeks, Phys. Rev. Lett. **40**, 733 (1978).
[15] S. F. Edwards and D. R. Wilkinson, Proc. R. Soc. London, Ser. A **381**, 17 (1982).
[16] M. Kardar, G. Parisi, and Y.-C. Zhang, Phys. Rev. Lett. **56**, 889 (1986).
[17] W. Wang and H. A. Cerdeira, Phys. Rev. E **47**, 3357 (1993).
[18] W. Wang and H. A. Cerdeira, Phys. Rev. E **52**, 6308 (1995).
[19] H. F. El-Nashar and H. Cerdeira, Phys. Rev. E **61**, 6149 (2000).
[20] C. M. Horowitz, R. A. Monetti, and E. V. Albano, Phys. Rev. E **63**, 066132 (2001).
[21] C. M. Horowitz and E. V. Albano, J. Phys. A **34**, 357 (2001).
[22] I. Irurzun, C. M. Horowitz, and E. V. Albano, Phys. Rev. E **72**, 036116 (2005).
[23] Y. P. Pellegrini and R. Jullien, Phys. Rev. Lett. **64**, 1745 (1990).
[24] Y. P. Pellegrini and R. Jullien, Phys. Rev. A **43**, 920 (1991).
[25] D. E. Wolf and F. Villain, Europhys. Lett. **13**, 389 (1990).
[26] S. Das Sarma and P. Tamborenea, Phys. Rev. Lett. **66**, 325 (1991).
[27] F. Family, J. Phys. A **19**, L441 (1986).
[28] A.-L. Barabási, R. Bourbonnais, M. Jensen, J. Kertész, T. Vicsek, and Y.-C. Zhang, Phys. Rev. A **45**, R6951 (1992).
[29] A.-L. Barabási and T. Vicsek, Phys. Rev. A **44**, 2730 (1991).
[30] J. Kertész and D. E. Wolf, J. Phys. A **21**, 747 (1988).
[31] J. Krug, Phys. Rev. Lett. **72**, 2907 (1994).
[32] Z.-W. Lai and S. Das Sarma, Phys. Rev. Lett. **66**, 2348 (1991).
[33] F. D. A. Aarão Reis, Phys. Rev. E **70**, 031607 (2004).